Tris(oxalato)phosphorus Acid and Its Lithium Salt

Ulrich Wietelmann,*[a] Werner Bonrath,[d] Thomas Netscher,[d] Heinrich Nöth,[b] Jan-Christoph Panitz,[a] and Margret Wohlfahrt-Mehrens[c]

Abstract: The conversion of three equivalents of anhydrous oxalic acid with phosphorus pentachloride yields tris(oxalato)phosphorus acid **1**, which crystallizes from diethyl ether solutions as protonated diethyl ether complex $[(Et_2O)_2H]^+[P(C_2O_4)_3]^-$. The superacidic compound can be used as catalyst for Friedel–Crafts-type reactions. Upon neutralization with lithium hydride, the lithium salt $Li[P(C_2O_4)_3]$ **2** is obtained, which is highly soluble in aprotic solvents and which exhibits a wide voltage window. Thus, the lithium compound is a promising candidate as electrolyte for high performance non-aqueous batteries.

Keywords: acidity · electrolytes · Friedel–Crafts reaction

Introduction

The development of new conducting salts for secondary lithium batteries requires compounds of excellent conductance and stability against oxidation. Besides $LiPF_6$, that is being used commercially, lithium tris(fluorocatecholato)phosphates show also promising properties.[1] There are two reasons, why these salts are advantageous i) the high symmetry of the anion makes them thermodynamically and kinetically quite stable, and ii) the negative charge is distributed over a large volume and this provides an opportunity for weak cation/anion interactions in solution. The disadvantage of the catecholatophosphates, is however, their comparatively high molecular weight. Reducing the molecular weight while maintaining the chelate effect to induce thermodynamic stability of the P–O bonds led us to investigate tris(oxalato)phosphates.

[a] Dr. U. Wietelmann, Dr. J.-C. Panitz
Chemetall GmbH, Trakehner Strasse 3
60487 Frankfurt (Germany)

[b] Prof. Dr. H. Nöth
Department Chemie, Universität München
Butenandtstrasse 5–13, 81377 München (Germany)

[c] Dr. M. Wohlfahrt-Mehrens
Zentrum für Sonnenenergie und Wasserstoff-Forschung
Helmholtzstrasse 8, 89081 Ulm (Germany)

[d] Dr. W. Bonrath, Dr. T. Netscher
Roche Vitamins AG
4070 Basel (Switzerland)

Results

Synthesis and properties: The conversion of dihydroxy compounds and different phosphorus raw materials such as halocyclophosphazenes or spiro[arylenedioxycyclophosphazenes],[2] phosphorylchloride,[3] phosphorus pentachloride[4] or even trivalent P-derivatives such as phosphorus trichloride[4] in the presence of amine bases yields hexacoordinated phosphate salts [Eq. (2)]. Likewise, the lithium salt of tris(*o*-phenylenedioxy)phosphate, synthesized by the conversion of PCl_5 with dilithio-*o*-phenylenediolate was shown to contain a hexacoordinate anion by spectroscopic methods ($\delta^{31}P = -82$ ppm).[5] In absence of bases, free acids may be formed and their structure depends on the complexing behaviour of the dihydroxy ligand. In the case of catechol as ligand, NMR investigations suggest only pentacoordination,[6] while its perfluorinated derivative is hexacoordinated,[1] see Table 1.

According to our knowledge, dicarboxylic acids have not yet been studied as ligands for the synthesis of tris(chelato)-phosphates.

Anhydrous oxalic acid reacts with PCl_5 in benzene under reflux conditions only with incomplete evolution of HCl gas (about 3 equiv per mol PCl_5). ^{31}P NMR measurements show that a mixture of P-containing species is formed. The main product is soluble in benzene, $\delta^{31}P = +5.1$ ppm. However, in polar, aprotic solvents HCl is evolved vigorously and quantitatively and tris(oxalato)phosphorus acid **1** is formed in good yield:[7]

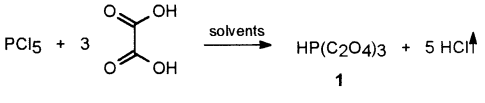

(1)

 DOI: 10.1002/chem.200305208

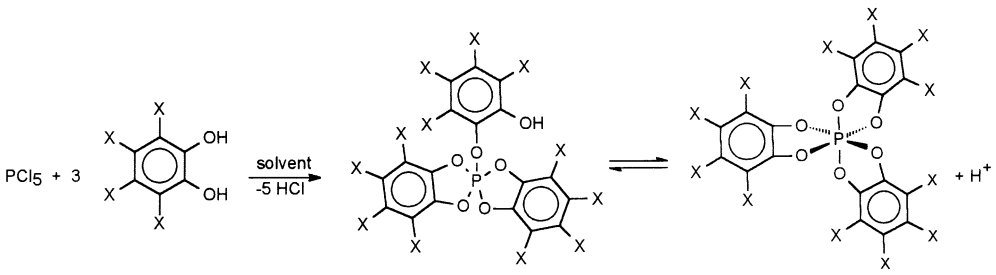

(2)

Table 1. Coordinated phosphate salts.

X	solvent[a]	δ^{31}P	Structure	Ref.
H	benzene	−29.65 (THF)	pentacoordinated	[6]
F	Et_2O	−71.35 (DMSO)	hexacoordinated	[1]

[a] For synthesis.

The most convenient solvent is dry diethyl ether, from which the acid crystallizes with 2 moles of solvent. The acid's solubility is only 0.04 mol kg^{-1} (1.2 wt %) at room temperature. Instead of Et_2O other aprotic solvents such as esters (e.g. ethyl acetate), carbonates (e.g. dimethyl carbonate, DMC or propylene carbonate, PC), or γ-butyrolactone are also suitable; however, in these solvents the acid is unstable. Interestingly, solvent mixtures, such as propylene carbonate/diethyl ether were found to be very suitable. 1–2 moles of diethyl ether should be present per mole of PCl_5.

Cyclic ethers such as tetrahydrofuran are not applicable, because they are readily cleaved within a few hours. Also, solutions in glymes are not stable: freshly prepared colorless solutions turn brown within minutes or hours.

The synthesis reported herein is not generally applicable to other dicarboxylic acids. As an example, from mixtures of 3 equiv of malonic acid and PCl_5 in diethyl ether only part of the expected HCl is liberated and NMR studies show no incidents for the formation of tris(malonato)phosphorus acid or its lithium salt after conversion with lithium bases (several signals in the ^{31}P NMR spectrum between 1 and 5 ppm).

Acid **1** shows only one signal in the ^{31}P NMR spectrum in all solvents tested so far (Et_2O; $CHCl_3$/Et_2O; PC/Et_2O; 1,2-dimethoxyethane (1,2-DME)/Et_2O) at about −141 ppm. The high field shift proves a phosphorus coordination number of six, that is, a structure similar to that of the perfluorocatechol compound mentioned above.

The crystalline **1**·2 Et_2O complex can be further dried in vacuo at about 30–60 °C, and one equivalent of diethyl ether is readily removed. Further removal of diethyl ether is impossible without decomposition of the tris(oxalato)phosphate anion. Figure 1 shows a DSC test of the crystalline **1**·2 Et_2O and **1**·Et_2O complexes.

$(Et_2O)_2H[P(C_2O_4)_3]$ melts at about 80 °C and starts to decompose exothermally at about 90 °C with $\Delta H_{decomp} = -265$ J g^{-1} (−117 kJ mol^{-1} for **1**). During this process noncondensable gases are released and at about 170 °C the pressure in the hermetically closed RADEX autoclave reaches almost 70 bar. The monoetherate melts at about 95 °C and starts to decompose at about 100 °C. Its molar heat of decomposition corresponds with that of the dietherate. Thermogravimetry shows a weight loss of 77 % up to 400 °C, while no further change of weight is observed until 500 °C. These data fit a decomposition reaction as shown in Equation (3) (theoretic weight loss 78.4 %) and the formation of a polyphosphoric acid residue:

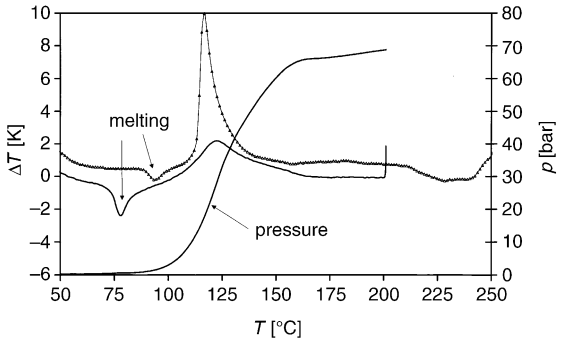

Figure 1. DSC data measured with RADEX system in closed autoclaves (▲ **1**·Et_2O, —— **1**·2 Et_2O).

$$n[HP(C_2O_4)_3 \cdot Et_2O] \rightarrow \mathbf{1} \cdot Et_2O \qquad (HPO_3)_n + n(3\,CO_2\uparrow + 3\,CO\uparrow + Et_2O\uparrow) \tag{3}$$

The spectroscopic data (see Table 2) of solutions in 1,2-DME and $CDCl_3$ support a symmetric hexacoordinated tris(oxalato)phosphate anion in the solution state. Compared with oxalic acid, the carbonyl ^{13}C NMR resonance is shifted 6 ppm to higher field. The IR data show a stronger double bond character of the C=O double bond (higher frequency).

In the ^{1}H NMR spectrum of the dietherate signals at δ 15.3 (in 1,2-DME) and 15.6 ppm (in $CDCl_3$) are observed for the acidic proton. This is a very significant downfield shift compared with oxalic acid, dissolved in 1,2-DME (11.3 ppm). Another characteristic feature is the lower field shift of the OCH_2 signal from 67.4 ppm (pure Et_2O) to 69.5 ppm for **1**·2 Et_2O in $CDCl_3$. In contrast, in the more polar 1,2-DME solvent the ether OCH_2 carbon is better

Table 2. Spectroscopic data for **1**·2 Et_2O and **1**·Et_2O.

Compound	Solvent	IR [cm^{-1}] (C=O)	$\delta^{31}P$	$\delta^{1}H$ (O···*H*)	$\delta^{13}C$ *C*=O	O–*C*H_2-	O–CH_2–*C*H_3
1·2 Et_2O	1,2-DME*	*1813*/1792/1748	−142.0	15.3	153.4	65.9	15.0
1·1 Et_2O	1,2-DME*	n.d.	−141.8	14.8	153.3	65.8	14.7
1·2 Et_2O	$CDCl_3$	n.d.	−140.7	15.6	153.3	69.5	13.9
1·1 Et_2O	$CDCl_3$	n.d.	−139.7	13.1	n.d.	67.8	14.6
2	1,2-DME*	1814/1794/1747	−141.8	n.a.	153.2	n.a.	n.a.
$H_2C_2O_4$	1,2-DME*	1772/1743	n.a.	11.3	159.3	n.a.	n.a.
Et_2O	–*	n.a.	n.a.	n.a.	n.a.	67.4	17.1

n.a. = not applicable n.d. = not determined * $CDCl_3$ added as reference.

shielded. This reflects interactions (or complex formation) of **1** with the stronger (compared with Et_2O) Lewis base 1,2-DME.

The NMR data of the monoetherate in 1,2-DME solution are only very slightly different from that of the diethetrate. In chloroform, **1**·Et_2O is nearly insoluble. The ^{31}P NMR resonance of the monoetherate is observed at marginally lower field, while the resonance of the acidic proton is shifted significantly to high field (from 15.6 in **1**·2 Et_2O to 13.1 ppm in **1**·Et_2O). This indicates interactions between the proton and the tris(oxalato)phosphate anion, thus the monoetherate's solution structure seems to be characterized by a dynamic equilibrium between the penta- and hexacoordinated forms **1a** and **1b**, see Equation (7). The spectroscopic data can also be explained by significant interactions between the cation $Et_2OH]^+$ and the phosphate anion, that is, the formation of contact ion pairs.

The extraordinary strength of acidity with concomitant low nucleophilicity of the corresponding anion qualifies **1** as an unusually well-suited catalyst for acid-induced chemical transformations. A remarkably efficient Friedel–Crafts-type alkylation reaction is depicted in Equation (4). The industrially important condensation reaction of trimethylhydroquinone **3** with (all-*rac*)-isophytol **4**, catalyzed by 0.5 mol% **1**, delivers (all-*rac*)-α-tocopherol (synthetic vitamin E, **5**) in up to 92% yield.[8] Investigations about further synthetic applications of **1** are ongoing.

Acid **1** can be neutralized with lithium bases to afford the lithium salt "LiTOP", **2**.[7] As the acid and the salt are not stable against hydrolysis, non-oxidic lithium bases (i.e., not LiOH or Li_2CO_3) have to be employed for this purpose.

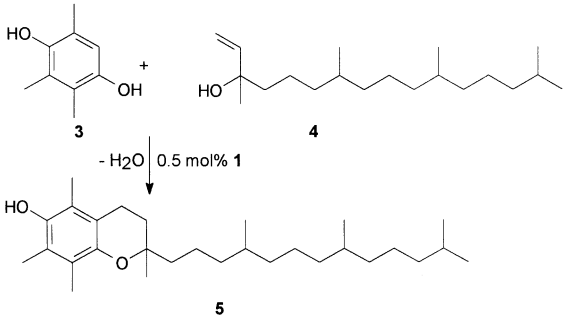

(4)

Lithium hydride is preferred because of its stability in ether solvents and the fact that no inconvenient by-products are formed [Eq. (5)]:

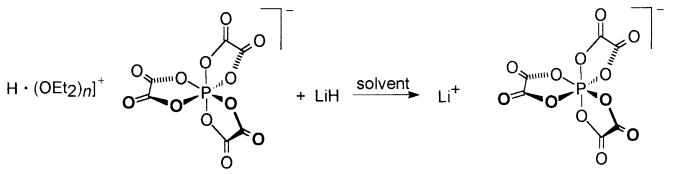

(5)

For reactions according to Equation (5) solvents such as diethyl ether or other polar aprotic solvents such as esters or carbonates can be employed. Another convenient salt synthesis starts from lithium oxalate, oxalic acid, and phosphorus pentachloride, as shown in Equation (6):

(6)

The lithium salt is slightly soluble in diethyl ether (0.09%), but dissolves excellently in more polar solvents (e.g. 43% in diethyl carbonate, 47% in THF, 53% in 1,2-DME). From dimethyl carbonate solutions a solvate **2**·DMC can be isolated. This complex is desolvated at about 107 °C (TGA measurements).

Pure, unsolvated **2** is stable until about 150 °C, but decomposes quickly above 190 °C. This decomposition process is exothermic and large quantities of gases (presumably CO and CO_2) are released. Figure 2 shows a RADEX experiment: the enthalpy of decomposition is measured to be approximately −127 $kJ\,mol^{-1}$, which is very close to the value of the free acid.

The spectroscopic data of the salt's anion (Table 2) are identical to that of the acid.

Electrochemical measurements: The cyclic voltammogram (CV) of LiTOP **2** in EC/DMC solvent mixture recorded against Pt electrodes is shown in Figure 3. In the first anodic sweep during the first cycle, a broad signal at ~5 V versus Li/Li^+ is observed. In the following cathodic sweep, a peak at 2.7 V versus Li/Li^+ is observed. In the following, a number of signals appear with lower current density. In the anodic sweep of the second and third cycle, an additional

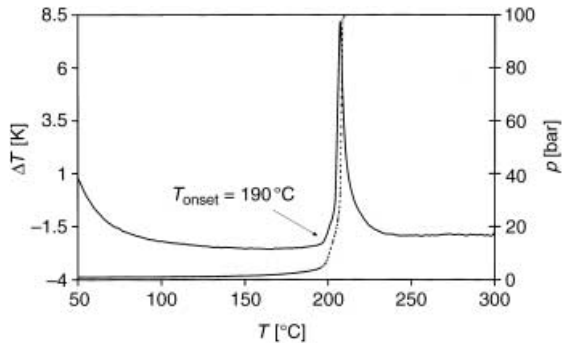

Figure 2. DSC and pressure data of **2** measured with RADEX system (—— DSC, ••••• pressure).

peak at 4.3–4.4 V versus Li/Li$^+$ is evident. The peak at 4.9 to 5.0 V increases in intensity. In the cathodic sweep of the second and third cycle, a split of the signal at 2.7 V into two signals located at 2.6 V and 2.1 V is recorded. We give the following tentative interpretation: the oxidation limit of the LiTOP based electrolyte is about 5.5 V. The signals at 5 and those in the 2–3 V range are due to impurities, most likely oxalic acid, hydrogenoxalate or oxalate, but a confirmation is pending.

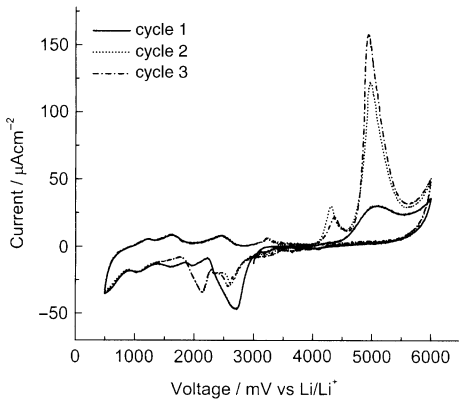

Figure 3. CV of LiTOP (**2**) electrolyte vs Pt WE electrode. The LiTOP was dissolved in EC/DMC solvent mixture. Sweep rate is 5 mV s^{-1}.

The CV against the carbon electrode is shown in Figure 4. In the first halfcycle, a signal at 2070 mV versus Li/Li$^+$ is observed, which does not appear afterwards (cf. inset of Figure 4). In the first halfcycle of Li insertion, a rather structureless *I*/*U* response is measured. In the following de-intercalation step, zero current is found at 320 mV and the de-intercalation peaks at 850 mV. In the second Li insertion step, the *I*/*U* response shows more structure than before. Upon de-insertion, zero current is again observed at 320 mV, but the peak current density is now observed at 890 mV. Thus, it is demonstrated that Li can be reversibly inserted into a carbon host. The nature of the signal is tentatively assigned to the reduction of the anion, possibly at one of the oxalate moieties.

Figure 5 compares the typical charge discharge curves of a carbon electrode in LiTOP electrolyte during the first and the following cycles. A small additional voltage plateau at

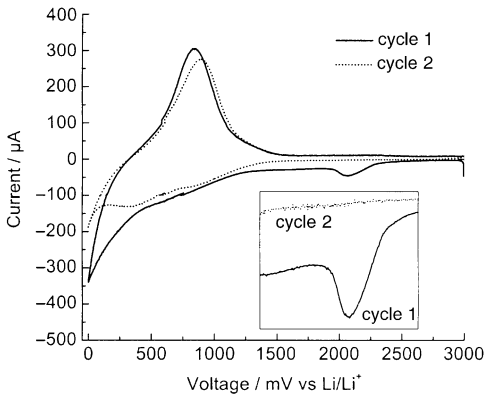

Figure 4. CV of LiTOP (**2**)–electrolyte against graphite.

2150 mV versus Li/Li$^+$ is observed in the first charge curve, which is in good agreement with the results obtained from CV measurements. This reduction process leads to a quite high irreversible capacity in the first cycle but does not affect the following cycles. The carbon electrode demonstrates a good electrochemical performance in terms of both recharge- and cycle-ability from the second cycle onwards. There are no changes of charge and discharge curves between two adjacent cycles after the first charge, which indicates a highly reversible lithium insertion into the carbon electrode.

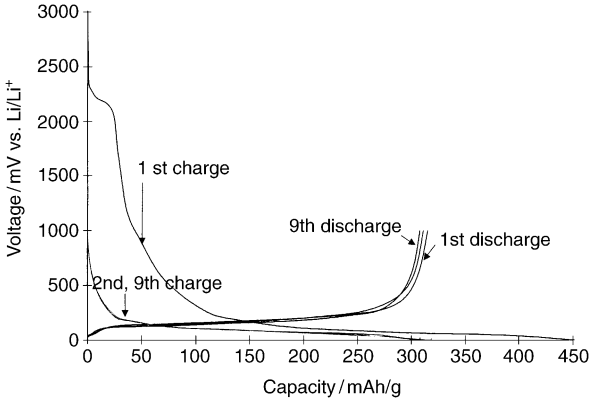

Figure 5. Charge and discharge curves of MCMB/Cu foil in LiTOP electrolyte; LiTOP was dissolved in EC/DMC (1:1) solvent mixture. The electrode was cycled between 0 and 1000 mV vs Li/Li$^+$, charge–discharge rate C/20; MCMB = mesocarbon microbeads.

Figure 6 shows the cycle-ability of a carbon electrode in LiTOP electrolyte. The electrode demonstrates full discharge capacity in the first cycle. No capacity fading is observed during subsequent cycles. The charge-discharge efficiency is nearly hundred percent from the second cycle, which implies that no electrolyte decomposition or other irreversible side reactions take place during lithium insertion.

Crystal structures: Tris(oxalato)phosphoric acid **1** crystallizes from diethyl ether as $[(Et_2O)_2H][P(C_2O_4)_3]$, **1**·2 Et_2O, in the centrosymmetric space group $P\bar{1}$ with two molecules in the unit cell. Figure 7 depicts the molecular structure with-

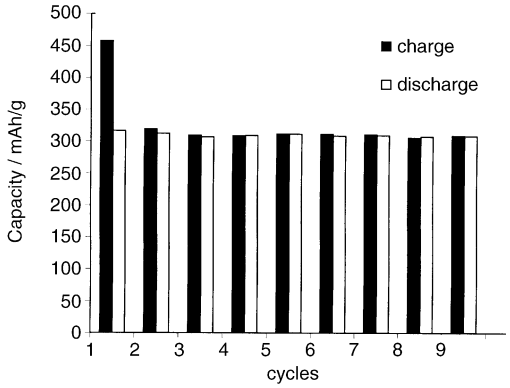

Figure 6. Galvanostatic cycle test of MCMB/Cu foil, lithium foil as reference and counter electrode in LiTOP electrolyte, LiTOP was dissolved in EC/DMC (1:1) solvent mixture. The cell was galvanostatically cycled between 0–1000 mV, charge, discharge rate C/20 MCMB = mesocarbon microbeads.

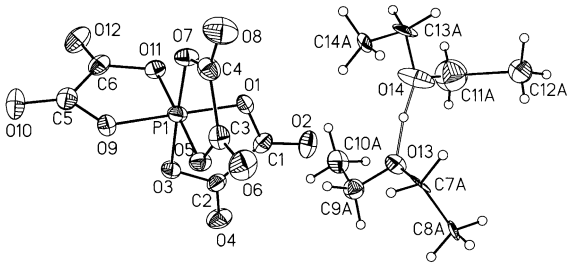

Figure 7. The molecular structure of $[(Et_2O)_2H][P(C_2O_4)_3]$ **1**·2 Et_2O. Only one of the two orientations of the ether molecules in the cation are shown. Thermal ellipsoids represent a 25% probability.

out showing the disorder of one of the diethyl ether molecules of the proton complex $[(Et_2O)_2H]^+$. As expected, the P–O bond lengths vary little and span the range from 1.684(2) to 1.705(2) Å with O-P-O bond angles from 88.4(2) to 91.8(2)° and 176.7(2) to 178.8(2)°, respectively. Thus, there is only little deviation from an octahedral geometry about the P atom. Particularly uniform are the C–C bond lengths of the oxalato unit (see Table 3). The endocyclic C–O bonds (1.324(4) to 1.347(4) Å) are significantly longer than the exocyclic C–O bonds (1.184(4) to 1.194(4) Å), which have definitely more double-bond character than the exocyclic C–O bonds. As expected, the oxalato groups are planar with dihedral angles between adjacent OCO unit varying only from 1.2 to 3.1°.

The cation $(Et_2O)_2H^+$ shows an almost symmetrical hydrogen bridge (H–O distances are 1.09 to 1.25 Å with an O–H·O bond angle of 172°). Both diethyl ether molecules show site disorder. Refinement in split positions lead to SOF values close to 0.5. In the final refinement these values were fixed to 0.5.

Relevant structural parameters are summarized in Table 3.

Compound $(MeO)_2CO$–$LiP(C_2O_4)_3$, **2**·DMC, crystallizes in the monoclinic system, space group $P2_1/n$ with $Z = 4$. As shown in Figure 8, there is a close Li–O contact. Expansion of the asymmetric unit reveals that each Li ion is coordinated to four oxygen atoms, three from three different oxalato groups of three $P(C_2O_4)_3$ anions. Consequently, each tris(oxalato)phosphate unit coordinates to three different Li ions. The Li–O bond to the dimethyl carbonate molecule is 0.01 Å shorter than those to the carbonyl groups, which are of equal lengths. The C=O bonds that coordinate to Li are slightly longer (av. 1.198 Å) than the non coordinated ones (av. 1.190 Å), but the difference is marginal considering the estimated standard deviations. The endocyclic C–O bonds are longer (av. 1.344 Å) when the exocyclic C=O group is not interacting with Li as compared with the other three endocyclic C–O bonds (av. 1.323 Å). This points to an uneven charge distribution within the oxalato units. However, there is no influence on the O-P-O bond angles which compare very nicely for the two compounds described here. The oxalate groups are almost planar; the interplanar O_2C bond angles for the three oxalato ligands vary from 1.6 to 3.2°.

Discussion

Synthesis and properties: The new acid tris(oxalato)phosphorus acid **1** can be synthesized in polar, aprotic solvents in

Table 3. Selected bond lengths [Å] and bond angles [°] for **1**·2 Et_2O and **2**·DMC.

1·2 Et_2O	**2**·DMC		**1**·2 Et_2O	**2**·DMC	
bond lengths					
P1–O1	1.696(2)	1.712(1)	P1–O3	1.694(2)	1.700(1)
P1–O5	1.705(2)	1.717(2)	P1–O7	1.684(2)	1.713(1)
P1–O9	1.691(2)	1.683(1)	P1–O11	1.686(2)	1.680(2)
C1–C2	1.515(5)	1.534(3)	C3–C4	1.516(5)	1.526(3)
C5–C6	1.515(5)	1.515(3)	C1–O1	1.336(4)	1.326(2)
C2–O3	1.328(5)	1.335(2)	C3–O5	1.324(4)	1.321(3)
C4–O7	1.327(4)	1.323(3)	C5–O9	1.347(4)	1.344(3)
C6–O11	1.335(5)	1.354(2)	C1–O2	1.191(4)	1.191(2)
C2–O4	1.184(4)	1.191(2)	C3–O6	1.188(3)	1.200(2)
C4–O8	1.191(4)	1.204(3)	C5–O10	1.178(4)	1.192(2)
C6–O12	1.191(4)	1.187(3)			
Li1–O8b		1.951(4)	Li1–O15		1.841(4)
Li1–O		1.953(4)	Li1–O7a		1.954(4)
bond angles					
O1-P1-O3	90.0(1)	90.17(6)	O5-P1-O7	89.9(1)	89.71(7)
O9-P1-O11	90.8(1)	90.81(7)	O1-P1-O7	88.4(1)	176.72(7)
O1-P1-O5	91.8(1)	176.72(7)	O1-P1-O9	178.8(1)	88.84(7)
O3-P1-O7	177.7(1)	88.33(6)	O3-P1-O9	88.8(1)	178.91(8)
O5-P1-O11	178.7(1)	178.83(7)	O5-P1-O9	88.5(1)	88.59(7)
O7-P1-O11	89.0(1)	89.31(7)	O1-C1-O2	123.9(4)	125.3(2)
O3-C2-O4	124.4(4)	125.8(2)	O5-C3-O6	125.4(3)	126.0(2)
O11-C6-O12	124.7(3)	124.0(2)	O9-C5-O10	124.6(4)	124.0(2)
O7-C4-O8	125.7(3)	123.9(2)	O6-Li1-O15		119.9(2)
O6D-Li1-O2		103.1(2)	O6D-Li1-O2		102.7(2)
O2-Li1-O8E		103.3(2)			

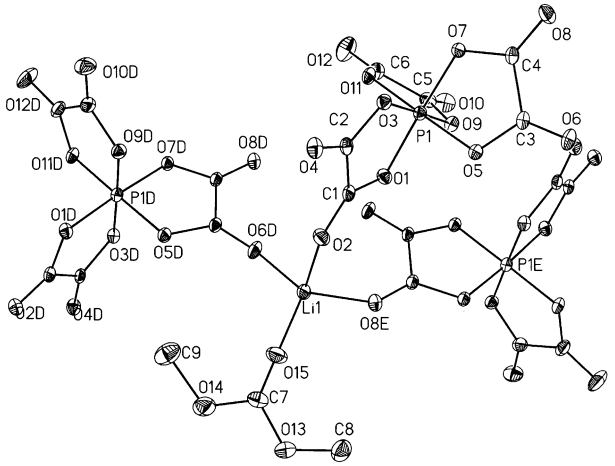

Figure 8. The coordination in compound **2**·DMC. Thermal ellipsoids are shown on a 5% probability scale.

high yields. Because of its high acidity, only few solvents are suitable as reaction media. Cyclic ethers, polyfunctional ethers or esters are attacked, and the acid is decomposed at RT within hours or days. Diethyl ether is specifically suitable to stabilize **1**; compound **1** forms two crystalline complexes with this solvent: a mono- and a dietherate. Spectroscopic studies show that the diethyl ether is protonated and the phosphate anion is not interacting with the proton. However, in solutions of the monoetherate **1**·Et_2O in non-coordinating solvents, there are significant cation/anion interactions (contact ion pairs) observed or there is an equilibrium between the five- and six-coordinated structures **1a** and **1b**, in which **1b** clearly prevails [Eq. (7)]:

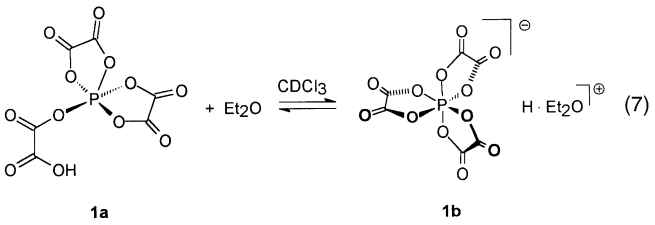

1a **1b** (7)

The highly symmetric anion of **1** is very efficiently delocalizing the negative charge due to the high number of carbonyl groups. Thus it is a strong non-nucleophilic soft base. The acidity of **1** is higher than that of the tris(catecholato)-phosphate, which is pentacoordinated in solvents with even relatively high donor capacity: Handa et al.[6] found a ^{31}P NMR shift of −29.65 ppm for the catechol compound in THF, which is clearly a value typical for pentacoordination.

The lithium salt **2** can be obtained from the acid **1** and an oxygen-free lithium base, most conveniently lithium hydride. It is stable until 150–190 °C and decomposes above this temperature, with evolution of large quantities of gases and formation of, presumably, lithium *poly*phosphate [Eq. (8)]:

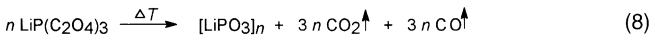

2 (8)

The decomposition is exothermic (ΔH_{decomp} = ca. −127 kJ mol^{-1}). In water, the lithium salt is not stable, but is hydrolyzed within minutes with formation of an unidentified main product with $\delta^{31}P = 3.8$ ppm. Compound **2** is very soluble in many aprotic polar solvents such as dimethyl carbonate, THF, ethyl acetate, dioxolane, acetone.

Structures: Compounds **1**·2Et_2O and **2**·DMC are the first examples of structurally characterized tris(oxalato)phosphates, where the P atoms are hexacoordinated. As already mentioned, hexacoordinated phosphates are known for a number of catecholato phosphates such as $Et_3NH[P(cat)_3]$ (cat = dianion of catechol),[9] $K[P(cat\text{-}3,6\text{-}(tBu)_2)_3]$,[10] $Et_2NH_2[P(cat\text{-}3,4,5,6\text{-}Cl_4)_3]$,[11] $[(Me_2NCHO)_2H][P(cat)_2(cat\text{-}3,4,5,6\text{-}Cl_4)]$,[12] $Et_3NH[P(cat\text{-}3,4,5,6\text{-}Cl_4)_2(O_2C_3H_6)]$,[13] $Et_3NH[P(cat\text{-}3,4,5,6\text{-}Cl_4)_2(OCH_2CMeEtCH_2O)]$,[14] $Et_3NH[P(cat\text{-}3,4,5,6\text{-}Cl_4)_2OCH_2CHtBuCH_2O)]$[14] or $[Et_3NH][P(cat)(OC_6H_5)_2(O_2C_2CF_3)_2)]$, **6**.[14] The structural parameters of these anions are similar to those found for **1**·2Et_2O and **2**·DMC, with some deviation for those anions that carry a propanediolate unit. In addition, there are also hexacoordinated phosphates known that carry a 2,2′-binaphtholato unit[15] or a bis(2,4-di-*tert*-butyl)phenolatosulfonate group besides pentafluorophenoxo units.[16] The compound that is closest to the oxalatophosphates is the bis(trifluoromethyl)-ethenediolate compound **6**, but due to three different ligands, the coordination around the P atom is much less symmetric than for **1**·2Et_2O and **2**·DMC. While there is no interaction between the cations and the anions of the hexacoordinated phosphates cited above, the slight differences found in the anions for compounds **1**·2Et_2O and **2**·DMC is a result of the interaction of the Li ion with the anion.

The proton of the bis(catecholato-3,4,5,6-tetrachlorocatecholato)phosphoric acid[13] is coordinated to the oxygen atoms of two molecules of dimethylformamide, and in this respect it is similar to that of **1**·2Et_2O. However, the oxonium ion $(Et_2O)_2H^+$ has also been found, and has been structurally characterized in $[(Et_2O)_2H]_2[Zn_2Cl_6]$[17] or $[(Et_2O)_2H][B(C_6F_5)_4]$[18] and $[Et_2O)_2H]_2[Ti_2Cl_7]$.[19] In each of these cases the proton does not interact with the anion. However, in contrast to **1**·2Et_2O, the tris(tetrafluorocatecholato)phosphoric acid, which like **1**·2Et_2O also crystallizes with two moles of diethyl ether[1] shows only the simple oxonium ion Et_2OH^+, that is the proton is evenly distributed between the two ether oxygen atoms.

Applications: The fact that tris(oxalato)phosphorus acid protonates diethyl ether and cleaves for example, THF proves it to be super acidic. This property qualifies it as active Brønsted acid promotor for acid-induced transformations, as has been demonstrated for a Friedel–Crafts-type condensation reaction [Eq. (4)].[8] Systematic investigations to compare the new fluorine-free acid with more standard ones such as HPF_6, CF_3SO_2OH, $(CF_3SO_2)_2NH$ are desirable in order to exploit its full synthetic scope.

The phosphate anion is characterized by a high symmetry and the negative charge is very efficiently distributed by the mesomeric delocalizing effect of the six carbonyl functions of the oxalate ligands. This is the basis of the high solubility

and conductivity of the lithium salt **2** in aprotic solvents. The anion also exhibits a remarkably high stability against anodic decomposition. Furthermore, according to first charge/discharge tests, lithium can be reversibly intercalated into graphitic materials from solutions of **2** in carbonate solvents. A reductive peak at about 2.15 V only in the first cycle suggests that the anion is involved in the so called formation process of the graphite anode, that is, the build-up of a passivating layer (SEI, solid electrolyte interface).

In this respect, it resembles other fluorine-free electrolytes like the lithium bis(oxalato)borate, which shows a formation peak at about 1.6–1.7 V.[20] This behaviour is in contrast to that of fluorinated salts such as $LiPF_6$ or $LiBF_4$, in which cases the SEI is mainly formed by the decomposition of ethylene carbonate, which is a prerequisite component of conventional liquid electrolytes for secondary lithium batteries with fluorinated conductive salts.[21,22] Thus, lithium tris(oxalato)phosphate potentially is a new candidate as conductive salt or additive for nonaqueous electrolytes in high energy nonaqueous batteries.

Experimental Section

General procedures: All manipulations were carried out under inert gas (preferably argon) in dried glassware equipment.

NMR spectra were recorded at RT on Bruker Advance DPX 250. All δ values are given relative to tetramethylsilane (^{1}H, ^{13}C) and external H_3PO_4/D_2O in the case of ^{31}P. As internal secondary reference $CDCl_3$ is employed ($\delta^1H = 77.0$ ppm, $\delta^{13}C = 128.0$ ppm). Infrared samples were measured as solutions in 0.05 mm cuvettes on a Nicolet Impact 400. Raman samples were filled into 5 mm NMR tubes and measured in solution on a Nicolet Raman 950.

Solvents were purified according to standard procedures or used as obtained. Anhydrous oxalic acid was dried over night at 80 °C and 50 mbar in a vacuum oven. PCl_5 was sieved through a 1 mm sieve before use. Lithium hydride powder from Chemetall has a D_{50} of about 0.1 mm.

DSC tests: Thermal analyses were performed with the RADEX system from company Systag, Switzerland. About 2–2.5 g of the substance to be analyzed were placed in hermetically closed 5 mL autoclaves or autoclaves connected with a pressure measuring device. The heating rate was normally 45 K h^{-1}.

X-ray structure determinations: Single crystals of compounds **1**·2 Et_2O and **2**·DMC (see Table 4) were covered with perfluoro ether oil and mounted on top of a glass fiber on the goniometer head of a Siemens P4 diffractometer equipped with a CCD area detector and cooled to −80 °C. $Mo_{K\alpha}$ radiation and a graphite monochromator was used. The unit cell dimensions were determined from the reflections collected on 15 frames each for five different settings. Data collection was performed in the hemisphere mode of the program SMART.[23] The data were reduced with the program SAINT and the structures solved by direct methods implemented in the program SHELXTL.[24] Non-hydrogen atoms were given anisotropic thermal parameters, while the hydrogen atoms were refined isotropically. The position and the U_i value of the oxonium hydrogen atom was freely refined. The site disordered ethyl group gave about equal occupancies for two orientations, and SOF was fixed to 0.5 in the final steps of refinement.

CCDC-211 204 (**1b**) and 211 203 (**2b**) contain the supplementary crystallographic data for this paper. These data can be obtained free of charge via www.ccdc.cam.ac.uk/conts/retrieving.html, or from the Cambridge Crystallographic Data Centre, 12 Union Road, Cambridge CB2 1EZ, UK; fax: (+44)1223–336033; or email: deposit@ccdc.cam.ac.uk.

Electrochemical investigations: The studies were carried out using solutions of LiTOP **2** in an ethylene carbonate (EC)/dimethyl carbonate (DMC) solvent mixture. The EC (battery grade, Digirena EC-20) was obtained from Honeywell and the DMC was obtained from Merck (Selectipur battery grade).

For the CV experiment, a solution of 10.5 wt% LiTOP in EC/DMC (1:1 *w*/*w*) was prepared, which was further dried using alumina (AluN, ICN Eschwege). One part of this solution was used to measure the CV against a Pt working electrode. A three-electrode cell without diaphragm was used. Two lithium strips (Chemetall, battery grade) fixed to nickel wire were used as counter and reference electrodes, respectively. Only the lithium strips were wetted by the solution. The cell was assembled in an argon-filled glove box (MB 200, M. Braun, München (Germany)); afterwards, it was connected to a Sycopel AEW-1000 electrochemical workstation. The CV was started by an anodic sweep from OCV to 6 V vs. Li/Li^+, followed by a cathodic sweep to 0.5 V vs. Li/Li^+, followed by an anodic sweep back to OCV. Three consecutive cycles were recorded, using a sweep rate of 5 mV s^{-1}. An additional CV experiment was performed using a graphite electrode and a Li counter electrode. The graphite electrode was prepared using a standard doctor blade coater. Graphite (Superior Graphite, Illinois) was dispersed in a solution of PVDF (polyvinylidene difluoride, Solvay 6020) in NMP (*N*-methyl pyrrolidin-2-one, Aldrich, Biotech grade) and coated on a copper current collector. After drying, electrodes were punched from the sheet and mounted in spring-loaded coin cells. For assembly, the cell was transferred to the glove box. A separator (Celgard 2400) and a Li metal disc were placed on top of the carbon electrode. After filling in the LiTOP-based electrolyte, the test cell was closed and transferred to the electrochemical workstation. The OCV of this cell was 3120 mV. Two complete cycles were recorded within the potential range OCV −5 mV, using a sweep rate of 200 μV s^{-1}. Because of the low sweep rate, potentials recorded are believed to be accurate, even without the use of a Li metal reference electrode.

Galvanostatic tests were performed in a three-electrode cell using lithium metal foil as counter and reference electrode. The carbon electrode was prepared by coating slurries of MCMB powder and PVDF dissolved in

Table 4. Crystallographic data of the acid **1**·2 Et_2O and its Li salt **2**·DMC.

	1·2 Et_2O	**2**·DMC
formula	$C_{14}H_{21}O_{14}P$	$C_9H_6LiO_{15}P$
F_w	444.27	392.05
cryst. size [mm]	0.50 × 0.60 × 0.70	0.27 × 0.22 × 0.34
cryst. system	triclinic	monoclinic
space group	$P\bar{1}$	$P2(1)/n$
a [Å]	7.4186(8)	12.2152(7)
b [Å]	11.285(1)	9.3340(5)
c [Å]	12.790(2)	13.3391(7)
α [°]	72.051(2)	90.00
β [°]	89.905(2)	104.251(1)
γ [°]	82.973(2)	90.00
V [Å^3]	1010.3(2)	1474.1(1)
Z	2	4
ρ_{calcd} [Mg m^{-3}]	1.444	1.767
μ [mm^{-1}]	0.205	0.273
$F(000)$	454	792
index range	$-7 \le h \le 9$	$-15 < h < 15$
	$-14 \le k \le 14$	$-11 < k < 11$
	$-15 \le l \le 15$	$-17 < l < 2$
2 θ [°]	57.74	58.14
T [K]	193(2)	193(2)
refl. collected	5698	8425
refl. unique	2990	2576
refl. observed (4σ)	2430	2112
R (int.)	0.0157	0.0780
no. variables	346	253
weighting scheme[a] x/y	0.1058/0.1893	0.0466/0.4657
GoF	1.068	1.027
final R (4σ)	0.0499	0.0356
final $wR2$	0.1478	0.0919
larg. res. peak [e Å^{-3}]	0.444	0.280

[a] $w^{-1} = \sigma^2 F_o^2 + (x\,P)^2 + y\,P$; $P = (F_o^2 + 2F_c^2)/3$.

NMP onto a copper foil. Celgard 2400 was used as separator. The cells were assembled in an argon-filled glove box and galvanostatically cycled between 0 and 1000 mV vs. Li/Li^+ with C/20 rate.

Synthesis: **$[(Et_2O)_2H][P(C_2O_4)_3]$ ($1{\cdot}2Et_2O$)**: Anhydrous oxalic acid (756 g, 8.40 mol) and dry diethyl ether (1100 g; water content $< 0.05\,\%$) were added while stirring into a 2 L double wall glass reactor equipped with corrosion resistant metal stirrer, condenser, distillation unit, Pt 100 thermocouple, gas volume measuring device, and a flask for solids addition. At temperatures between 20 and 25 °C, only parts of the acid dissolved.

After about 10 min stirring, lump-free phosphorus pentachloride (564 g, 2.71 mol) was added portion wise over a period of about 90 minutes. During the first quarter of administering, the temperature rose due to the exothermic reaction. Initially, the hydrogen chloride by-product dissolved in the ether, but after about 10–20 g of PCl_5 addition, HCl gas evolved and mild foaming was sometimes observed. By cooling, the reaction temperature was kept between 20 and 30 °C. After about 150 g of PCl_5 had been added, the reaction temperature decreased due to the endothermic vigorous evolution of gaseous HCl. At this stage, the mixture was heated in order to keep the temperature above ca. 20 °C. Two liquid phases were formed and the heavier one crystallized during the second half of the addition.

After the PCl_5 addition was completed, about 160 L of HCl were generated. In order to complete the gas evolution, the reaction mixture was heated under reflux with vigorous stirring by raising the temperature of the heating mantle to 40–43 °C for 1–2 h. Thereafter as much diethyl ether was boiled off as possible while stirring (about 500 mL). In order to reduce the content of chloride impurities, the solids were then dried under vacuum (membrane pump).

After this procedure, the white to slightly pale solids were redispersed in fresh diethyl ether (about 500–800 g). The slurry which forms was poured onto a filter unit and washed three times with diethyl ether. The crystalline solid was vacuum dried at RT for about two hours. yield: 910 g **1**·2 Et_2O (75 %); m.p. ≈80 °C (decomp); elemental analysis calcd (%) for P: 6.97, Cl^-: 0; found: P (ICP) 6.97, Cl^- (argentometric): 0.11; NMR ($CDCl_3$): δ^1H = 1.47 (t, H_3C), 4.08 (q, CH_2), 15.5 (s, $H{\cdot}Et_2O$); $\delta^{13}C$ = 14.39, 69.98 (Et_2O), 153.79 (ligand); $\delta^{31}P$ = −140.7; NMR (1,2-DME/C_6D_6): δ^1H = 0.96 (t, H_3C), 2.3–4.0 (1,2-DME and H_2C), 15.6 (s, $H{\cdot}Et_2O$); $\delta^{13}C$ = 14.86, 65.77 (Et_2O), 153.2 (ligand); $\delta^{31}P$ = −141.97; IR (5 % solution in 1,2-DME):$\tilde{\nu}$ = 1813 (s), 1792 (sh), 1748 cm^{-1} (w); Raman (NMR tube, 5 % solution in 1,2-DME): $\tilde{\nu}$ = 1842, 1799 cm^{-1} (both w).

Remarks: **1**·2 Et_2O was not stable in 1,2-DME over longer periods of time, therefore solutions have to be measured quickly (within 1–2 h).

$[Et_2OH]$ $[P(C_2O_4)_3]$ ($1{\cdot}Et_2O$): crystalline **1**·2 Et_2O was kept for 1–2 h at 50–60 °C under vacuum (< 1 mbar). Elemental analysis calcd (%) for P: 8.37; found: P 8.36.

$Li[P(C_2O_4)_3]$ (crude 2, step 1): In a 1 L flask equipped with a stirrer, condenser, thermocouple and solids addition flask **1**·2 Et_2O (250 g, 0.56 mol) was suspended in dry diethyl ether (500 mL). To this suspension lithium hydride powder (5.6 g, 0.71 mol) was added under vigorous stirring at RT. Rapid hydrogen evolution was observed and care had to be taken in order to prevent foaming. After complete addition, the mixture was heated under reflux for 1–3 h until no more hydrogen evolution was observed. The mixture was evaporated to dryness at 30–80 °C with a rotary evaporator to yield a white to slightly greyish powder (160–175 g). ***Caution***: The solid still contains excess lithium hydride.

Step 2—Purification of crude 2: The crude reaction product of Step 1 was dissolved in dry diethyl carbonate (addition of the raw solid to stirred solvent at about 20–50 °C, so that an about 30 % solution was formed). Whereas **2** dissolved quickly, LiH and other impurities did not dissolve and were removed by filtration over a G4 glass filter frit. The clear filtrate obtained was vacuum evaporated (60–75 °C, 80–100 mbar).

When the salt concentration exceeded about 35 %, pure **2** crystallized in the form of coarse colourless crystals. The evaporation was continued as long as the stirring was not affected. Then, the suspension was cooled to RT and poured onto a filter frit (G2 or G3). The crystals were washed with a small quantity of diethyl carbonate (DEC), then with *tert*-butyl methyl ether. Finally, the salt was vacuum dried at 50–90 °C for about one hour. Yield: 85–120 g.

From the mother liquor another 10–30 % **2** could be isolated. The chloride impurity level was typically between 50 and 300 ppm. It was reduced by repeated recrystallizations. NMR (1,2-DME/C_6D_6): δ^1H = only signals from 1,2-DME (3.11, 3.28); $\delta^{13}C$ = 58.22, 71.68 (1,2-DME), 153.17 (*C*=O); $\delta^{31}P$ = −141.8; IR (5 % solution in 1,2-DME): $\tilde{\nu}$ = 1814 (s), 1794 (sh), 1747 cm^{-1} (w); Raman (NMR tube, 5 % solution in 1,2-DME): $\tilde{\nu}$ = 1841, 1799 cm^{-1} (both w).

$(MeO)_2CO{\cdot}Li[P(C_2O_4)_3]$ (2·DMC): Compound **2** was added to dry dimethyl carbonate so that an ~35 % suspension was formed. If turbid, the resulting solution was filtered over a G4 glass frit. Next, the clear filtrate was concentrated under vacuum (200–500 mbar) at 50–70 °C, until white crystals formed. The solution was then cooled slowly to 0 °C, and the solid was isolated by filtration. Yield: 40–60 % of theory; elemental analysis calcd (%) for P 7.90, Li 1.77; found P (ICP) 7.74, Li (ICP) 1.74. The solubility of **2** in dimethyl carbonate was as follows: *T* [°C] (conc. [wt. %]): 0 (40), 25 (41), 50 (43), 70 (44).

[1] M. Eberweis, A. Schmid, M. Schmidt, M. Zabel, T. Burgemeister, J. Barthel, W. Kunz, H. J. Gores, *J. Electrochem. Soc. Interface*, in press.
[2] H. R. Allock, R. L. Kugel, G. Y. Moore, *Inorg. Chem.* **1975**, *14*, 2831–2837.
[3] M. Gallagher, *J. Chem. Soc. Chem. Commun.* **1976**, 321–322.
[4] J. Gloede, H. Gross, *Tetrahedron Lett.* **1976**, *17*, 917–920.
[5] D. Hellwinkel, H.-J. Wilfinger, *Chem. Ber.* **1970**, *103*, 1056–1064.
[6] M. Handa, M. Suzuki, J. Suzuki, H. Kanematsu, Y. Sasaki, *Electrochem. Solid State Lett.* **1999**, *2*, 60–62.
[7] U. Lischka, K. Schade, U. Wietelmann, DE 19933898, Chemetall GmbH, **1999**.
[8] W. Bonrath, T. Netscher, U. Wietelmann, EP 1227089 A1, Roche Vitamins AG, **2001**; presentation at XXXVI. Jahrestreffen Deutscher Katalytiker, 19–21 March 2003, Weimar, Germany, P 121.
[9] E. C. Bissel, *J. Am. Chem. Soc.* **1973**, *95*, 3154.
[10] D. S. Yufit, Yu. T. Struchkov, A. I. Matrosov, D. N. Lobenov, N. V. Matrosoa, M. I. Kabatchnik, *Zh. Strukt. Khim.* **1988**, *29*, 131.
[11] I. V. Sherchenko, A. Fischer, P. G. Jones, R. Schmutzler, *Chem. Ber.* **1992**, *125*, 1325.
[12] J. Lacour, C. Ginglinger, C. Grivet, G. Bernadinelli, *Angew. Chem.* **1997**, *109*, 622; *Angew. Chem. Int. Ed. Engl.* **1997**, *36*, 608.
[13] A. Slowonska, J. Kowara, F. R. Kaminski, G. Bijacz, M. W. Wieczowek, *J. Org. Chem.* **2000**, *65*, 304.
[14] R. Sarma, F. Ramirez, B. McKeever, J. F. Maricek, V. A. V. Prasad, *Phosphorus Sulfur Relat. Elem.* **1979**, *5*, 323.
[15] J. Lacour, A. Londez, G. Gouglon-Ginglinger, V. Buss, G. Bernadinelli, *Org. Lett.* **2000**, *2*, 4185.
[16] P. Sool, A. Chandrasekaran, R. O. Day, R. R. Holmes, *Inorg. Chem.* **1998**, *37*, 6329; A. Chandrasekaran, R. O. Day, R. R. Holmes, *Inorg. Chem.* **1997**, *36*, 2578.
[17] I. V. Lyudkoskaya, M.Yu. Antigia, Yu. T. Struchkov, A. M. Nefedov, *Izv. Akad. Nauk SSSR, Ser. Khim.* **1985**, 79.
[18] P. Jutzi, C. Müller, A. Stammler, H. G. Stammler, *Organometallics* **2000**, *19*, 1442.
[19] S. Rannabauer, T. Habereder, H. Nöth, W. Schnick, *Z. Naturforsch.* **2003**, *58*, 745–750.
[20] K. Xu, S. Zhang, T. R. Jow, *Electrochem. Solid-State Lett.* **2003**, *6*, A117–A120.
[21] D. Aurbach, B. Markovsky, I. Weissmann, E. Levi, Y. Ein-Eli, *Electrochim. Acta* **1999**, *45*, 67–86.
[22] A. M. Andersson, M. Herstedt, A. G. Bishop, K. Edström, *Electrochim. Acta* **2002**, *47*, 1885–1898.
[23] SMART, programs for data collection, Siemens Analytical Instruments, Madison, Version 5.1.
[24] SHELX TL, W. G. Sheldrick, University of Göttingen, **1997**.

Received: June 5, 2003 [F5208]

Published online: March 10, 2004